Statistical Atlas of Human Cardiac Fibers: Comparison with Abnormal Hearts

Herve Lombaert[1,2], Jean-Marc Peyrat[4], Laurent Fanton[3], Farida Cheriet[2], Hervé Delingette[1], Nicholas Ayache[1], Patrick Clarysse[3], Isabelle Magnin[3], Pierre Croisille[3]

[1] INRIA, Asclepios Team, Sophia-Antipolis, France
[2] École Polytechnique de Montréal, Canada
[3] CREATIS, Université de Lyon, France
[4] Siemens Molecular, Oxford, UK

Abstract. Criteria of normality of the cardiac fibers are important in cardiomyopathies. In this paper, we investigate the differences in the cardiac fiber structures between 10 hearts classified as healthy and 6 hearts classified as abnormal, and determine if properties of the cardiac fiber structures can be discriminants for abnormality. We compare the variability of the fiber directions from abnormal hearts to an atlas of healthy hearts. The human atlas of the cardiac fiber structures is built with an automated framework based on symmetric Log-domain diffeomorphic demons. We study the angular variability of the different fiber structures. Our preliminary results might suggest that a higher variability of the fiber structure directions could possibly characterize abnormality of a heart.

1 Introduction

Cardiovascular diseases are by far the number one killer in the US with over 930,000 deaths annually and 71 millions, more than a fifth of the population, live with a form of cardiovascular disease [20]. The characterization of the consequences lead by specific cardiopathies is essential to a better diagnosis and a better treatment of these diseases. Among the possible causes, the differences in the cardiac fiber architecture could be an promising topic. The heart is composed of myocardial fibers organized in a complex laminar structure [18,10], and the cardiac fiber structures have an important role in electrophysiology [8], in mechanical functions [4], and in remodeling [23] of the heart. Changes in the fiber structures are for instance inherent in myocardial hypertrophy [9,19,6]. Myocardial disarray, or disorganisation of the fibers, is also still the focus of contentious studies [2]. The question of normality of the cardiac fiber structures arises when trying to assess the role of myocardial disarray in cardiomyopathies. In this paper, we try to assess whether there is a difference in the cardiac fiber structures between hearts classified as normal and hearts considered as abnormal.

The directions of the fiber structures and their variability can be measured with Diffusion Tensor Imaging (DT-MRI). A human atlas of the cardiac fiber

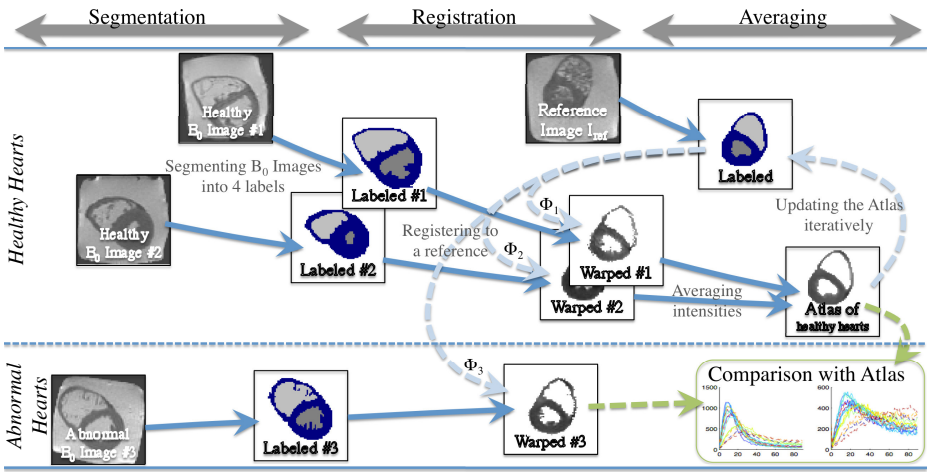

Fig. 1. *Construction of the healthy atlas*: The myocardia are segmented. Images are then aligned and registered non-rigidly toward a reference image. The atlas is constructed iteratively by averaging acquired images in the average heart shape. *Comparison with the atlas*: Abnormal hearts are registered to the average healthy heart. The cardiac fiber structures of each abnormal heart are compared with the structures of the average healthy heart.

structures from DT-MRI [12,13] has recently been built with 10 healthy *ex vivo* hearts. We register 6 *ex vivo* hearts classified as abnormal to the atlas of healthy hearts and analyze the angular differences between the fiber structure directions of the abnormal hearts and the ones of the average healthy heart. The statistical study shows that the directions of the cardiac fiber structures vary more in abnormal hearts than in healthy hearts. The preliminary results might suggest that a higher variability of the fiber structure directions could possibly characterize abnormality.

2 Material and Method

2.1 Dataset

The human dataset [5,16] consists of 10 healthy and 6 abnormal *ex vivo* human hearts acquired during forensic autopsies. All cases are from extra cardiac sudden deaths. However, the true nature of deaths is not available. The images have been acquired on a 1.5T MR scanner (Avanto Siemens), all within 24 hours after death and prior to the examination by the pathologist, with a bipolar echo planar imaging using 4 repetitions of 12 gradient images. The diffusion-weighted images, from which are estimated the diffusion tensors, are of size 128x128x52 with an isotropic resolution of 2 mm. Criteria of abnormality [17] are based on the heart weight (with given permitted weight limits within the 95% percentile),

the septal thickness (with a maximal thickness defined at 12 mm for women and 14 mm for men), and on subsequent pathology examination.

2.2 Registration of Abnormal Hearts

The atlas of diffusion tensors is constructed using the automated framework described in [12]. The method is summarized in Fig. 1 and has four steps. The myocardium is segmented [3] and its mask is used to guide the nonrigid pairwise registration [21,22,14]. All hearts are registered to an initial reference image, which is updated toward the morphological average of all hearts [7]. Once the transformations of all hearts toward the average cardiac shape are computed, the diffusion tensors are warped [15] to the morphological atlas.

The processing of abnormal hearts is performed within the same framework [12]. Firstly, the myocardia of the abnormal hearts are segmented using a minimal user interaction. Secondly, their masks are registered to the newly computed average healthy heart. The diffusion tensors are warped accordingly to the shape of the average healthy heart.

2.3 Comparison with Abnormal Hearts

The diffusion tensors fields from all hearts, $\{\mathbf{D}^{(i)}\}_{i=1\ldots N}$ (with $N = 10$ healthy + 6 abnormal hearts), are warped to the morphological average of the healthy hearts (i.e., in a common reference). The Log-Euclidean metric [1] is used to compute efficiently the average diffusion tensor of the healthy hearts (hearts #1 to #10) with the Fréchet mean, $\overline{\mathbf{D}} = \exp\left(\frac{1}{10}\sum_{i=1}^{10}\log(\mathbf{D}^{(i)})\right)$.

The eigendecomposition of the diffusion tensor matrix $\overline{\mathbf{D}}$ gives the principal directions $\mathbf{v}_{1,2,3}$ describing the fiber structures. More precisely, the first eigenvector $\mathbf{v}_1$ gives the fiber orientation, the second eigenvector $\mathbf{v}_2$ is believed to lie within the laminar sheet and to be perpendicular to the fiber, and the third eigenvector $\mathbf{v}_3$ is assumed to give the normal of the laminar sheet.

The abnormal hearts are compared with the average healthy heart by measuring the angular deviations of the fiber structures of each heart with the average heart. The angle θ between the direction of an eigenvector $\mathbf{v}_j$ of the i^{th} heart and the direction of the corresponding average eigenvector $\overline{\mathbf{v}}_j$ is defined between 0° and 90° with:

$$\theta_j^{(i)} = \arccos\left(\frac{|\mathbf{v}_j^{(i)} \cdot \overline{\mathbf{v}}_j|}{\| \mathbf{v}_j^{(i)} \| \| \overline{\mathbf{v}}_j \|}\right) \tag{1}$$

The absolute value of the dot product removes the inherent ambiguity in the orientation of the eigenvectors (i.e., $|a \cdot b| = |a \cdot (-b)|$).

3 Results

We study the deviation of the fiber structures of each heart (healthy and abnormal) to the average structures of the healthy hearts (i.e., to the atlas). The

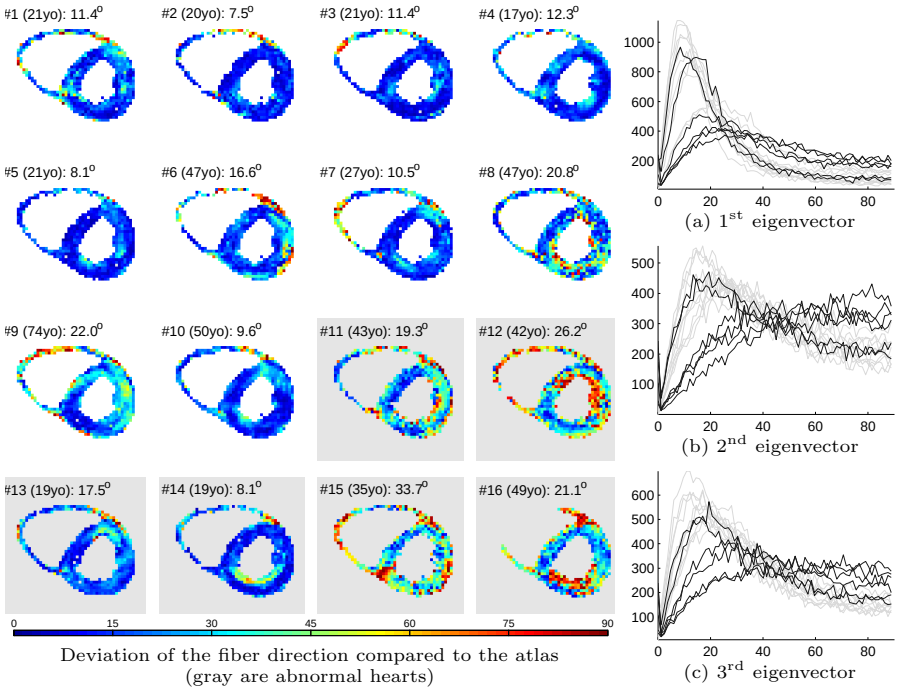

Fig. 2. *(Left)* Deviation of the fiber direction of each heart to the atlas of healthy hearts. Coloring is the angular difference in degree. Abnormal hearts are with gray background. The age of each subject is provided in each sub figure. *(Right)* Histograms of the angular variability (in degrees) of *(a)* the 1st eigenvector, *(b)* 2nd eigenvector, and *(c)* 3rd eigenvector (abnormal hearts in dark lines, healthy hearts in light lines).

structures in the healthy hearts are, as expected, very similar to the atlas. The histograms of the angular differences of the first, second, and third eigenvectors of the healthy hearts to the atlas (gray curves in Fig. 2) show average modes of respectively (i.e., the curves are peaking at) $\overline{\theta}_1 = 13.03°$, $\overline{\theta}_2 = 21.76°$, and $\overline{\theta}_3 = 15.77°$. Abnormal hearts show by contrast fiber structures that have larger deviations to the atlas of healthy hearts. The histograms of the angular differences of structures show higher modes in abnormal hearts (black in Fig. 2), with a deviation of $\overline{\theta}_1 = 20.96°$ for the fibers (i.e., first eigenvector) and of $\overline{\theta}_2 = 48.21°$ and $\overline{\theta}_3 = 34.36°$ for the laminar sheets (i.e., second and third eigenvector). The visualization of the angular difference in a slice of each heart shows large discrepancies in the left ventricle with localized high-variability areas for patient #12, #15, and #16 (shown in the sub-figures of Fig. 2 with gray backgrounds). This is again confirmed when visualizing the angular difference of the second and third eigenvectors (i.e., the laminar sheets). It is to note that the registration of the right ventricle (which exhibited a very small volume) failed for the

last patient (#16). The patients #13 and #14, even if classified as abnormal, presented consistently very small deviations to the average fiber structures of the healthy atlas (Fig. 2).

4 Discussion and Conclusion

The question whether the variability of the cardiac fiber structures is a marker to normality or abnormality is relevant to the study of many cardiomyopathies, including left ventricular hypertrophy or myocardial disarray. In this paper, we compared the structural changes between a population of abnormal hearts and of healthy hearts. It was shown that the three eigenvectors of the diffusion tensors have measurable differences between abnormal hearts and healthy hearts. When compared to an atlas of healthy hearts, the fibers of abnormal hearts showed an angular difference of 20.96°, while the fibers of healthy hearts showed less deviation with 13.03°. The laminar sheets also showed a greater deviation and a greater variability in abnormal hearts than in healthy hearts. Even though the laminar sheet is known to be more variable than the fiber structure in humans [12], the difference in both populations is non negligible (deviation of the laminar sheet normal of 34.36° in abnormal hearts compared to 15.77° in healthy hearts). The abnormal hearts also experience a large fiber angle difference around trabeculae areas. A localized study might reveal the origin of such large deviance.

Nonetheless, two outliers are present (hearts #13 and #14 as shown in Fig. 2). They were initially classified as abnormal even though their cardiac fiber structures are very similar to the average healthy heart (deviation of 17° and 8°). We hold the attention on the age of both subjects, both very young (19 years old). Furthermore, the modes in healthy hearts, i.e., the peaks of the histograms in Fig. 2(a), also show that the cardiac fibers are less variable in younger subjects than in older subjects. Age is thought to have an impact in the fiber structure of skeletal muscles [11]. No study has yet been performed in cardiac muscles. For that matter, the mode of the angular differences of the first eigenvector (i.e., the fiber direction) was plotted against the age of each subject (Fig. 3). The correlation factor between age and fiber variability is 0.73 when considering only the 10 healthy hearts (with a low p-value of 0.016). When considering only the abnormal hearts, the correlation factor is higher at 0.86 (with a p-value of 0.029). The estimated least-square fit lines of both population are overlaid in Fig. 3. Before hypothesizing that the variability of the fiber directions increases faster with age in abnormal hearts, many unknown parameters should be considered firstly (for instance, the distinction between primitive

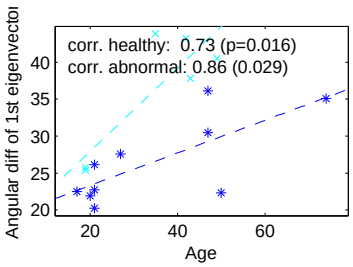

Fig. 3. Possible correlation between the age and the fiber variability (healthy hearts in blue with a correlation factor $\rho = 0.73$, abnormal in cyan with $\rho = 0.86$).

hypertrophy or secondary hypertrophy, known to occur in old subjects, is here unknown).

In conclusion, our study comparing a population of abnormal hearts and of healthy hearts showed that there are observable differences in the fiber directions in both populations. Abnormal hearts have fiber directions that are more variable and that are on average 20.96° different from the average healthy heart. Future studies will include additional hearts in order to further study these preliminary findings.

Acknowledgment

The authors wish to acknowledge the members of the Asclepios Team. The project was supported financially by the National Science and Engineering Research Council of Canada (NSERC), the Michael Smith Scholarship (CGS-MSFSS), and the EGIDE/INRIA Scholarship.

References

1. V. Arsigny, P. Fillard, X. Pennec, and N. Ayache. Log-Euclidean metrics for fast and simple calculus on diffusion tensors. *Magnetic Resonance in Medicine*, 56(2):411–421, 2006.[3]
2. A. E. Becker and G. Caruso. Myocardial disarray. a critical review. *British Heart Journal*, 47(6):527–538, June 1982.[1]
3. Y. Boykov and M.-P. Jolly. Interactive Organ Segmentation Using Graph Cuts. In *Medical Image Computing and Computer Assisted Intervention*, pages 276–286, 2000.[3]
4. K. D. Costa, J. W. Holmes, and A. D. Mcculloch. Modelling cardiac mechanical properties in three dimensions. *Mathematical, Physical and Engineering Sciences*, 359(1783):1233–1250, 2001.[1]
5. C. Frindel, M. Robini, P. Croisille, and Y.-M. M. Zhu. Comparison of regularization methods for human cardiac diffusion tensor MRI. *Med. Im. An.*, 13(3), 2009.[2]
6. S. Grajek, M. Lesiak, M. Pyda, M. Zajac, St Paradowski, and E. Kaczmarek. Hypertrophy or hyperplasia in cardiac muscle. post-mortem human morphometric study. *European Heart Journal*, 14(1):40–47, January 1993.[1]
7. A. Guimond, J. Meunier, and J. P. Thirion. Average Brain Models: A Convergence Study. *Computer Vision and Image Understanding*, pages 192–210, 2000.[3]
8. D. A. Hooks, K. A. Tomlinson, S. G. Marsden, I. J. LeGrice, B. H. Smaill, A. J. Pullan, and P. J. Hunter. Cardiac Microstructure: Implications for Electrical Propagation and Defibrillation in the Heart. *Circulation Research*, 91(4):331–338, 2002.[1]
9. H. T. Karsner, O. Saphir, and T. W. Todd. The state of the cardiac muscle in hypertrophy and atrophy. *The American journal of pathology*, 1(4), July 1925.[1]
10. I. J. LeGrice, B. H. Smaill, L. Z. Chai, S. G. Edgar, J. B. Gavin, and P. J. Hunter. Laminar structure of the heart: ventricular myocyte arrangement and connective tissue architecture in the dog. *The American journal of physiology*, 269(2), 1995.[1]
11. J. Lexell and C. C. Taylor. Variability in muscle fibre areas in whole human quadriceps muscle: effects of increasing age. *Journal of anatomy*, 174:239–249, February 1991.[5]

12. H. Lombaert, J.-M. Peyrat, P. Croisille, S. Rapacchi, L. Fanton, P. Clarysse, H. Delingette, and N. Ayache. In *Function Imaging and Modeling of the Heart*, volume 6666, pages 171–179, 2011.[2, 3, 5]
13. H. Lombaert, J.-M. Peyrat, S. Rapacchi, L. Fanton, H. Delingette, P. Croisille, P. Clarysse, and N. Ayache. In *ISMRM*, 2011.[2]
14. T. Mansi, X. Pennec, M. Sermesant, H. Delingette, and N. Ayache. iLogDemons: A Demons-Based registration algorithm for tracking incompressible elastic biological tissues. *International Journal of Computer Vision*, pages 1–20, 2010.[3]
15. J.-M. Peyrat, M. Sermesant, X. Pennec, H. Delingette, C. Xu, E. R. McVeigh, and N. Ayache. A Computational Framework for the Statistical Analysis of Cardiac Diffusion Tensors: Application to a Small Database of Canine Hearts. *IEEE Transactions on Medical Imaging*, 26(11):1500–1514, 2007.[3]
16. S. Rapacchi, P. Croisille, V. Pai, D. Grenier, M. Viallon, P. Kellman, N. Mewton, and H. Wen. Reducing motion sensitivity in free breathing DWI of the heart with localized Principal Component Analysis. In *ISMRM*, 2010.[2]
17. M. Silver, A. I. Gotlieb, and F. R. Schoen. *Cardiovascular Pathology*. Churchill Livingstone, 3 edition, 2001.[2]
18. D. D. Streeter, H. M. Spotnitz, D. P. Patel, J. Ross, and E. H. Sonnenblick. Fiber Orientation in the Canine Left Ventricle during Diastole and Systole. *Circulatory Research*, 24(3):339–347, 1969.[1]
19. F. Tezuka. Muscle fiber orientation in normal and hypertrophied hearts. *The Tohoku journal of experimental medicine*, 117(3):289–297, November 1975.[1]
20. T. Thom, N. Haase, W. Rosamond, V. J. Howard, J. Rumsfeld, T. Manolio, Z.-J. Zheng, K. Flegal, C. Odonnell, S. Kittner, D. Lloyd-Jones, D. C. Goff, and Y. Hong. Heart disease and stroke statistics–2006 update. *Circulation*, 113:85–151, 2006.[1]
21. T. Vercauteren, X. Pennec, A. Perchant, and N. Ayache. Symmetric Log-Domain Diffeomorphic Registration: A Demons-Based Approach. In *Medical Image Computing and Computer Assisted Intervention*, pages 754–761, 2008.[3]
22. T. Vercauteren, X. Pennec, A. Perchant, and N. Ayache. Diffeomorphic demons: efficient non-parametric image registration. *NeuroImage*, 45(1):S61–S72, March 2009.[3]
23. M.-T. Wu, W.-Y. I. Tseng, M.-Y. M. Su, C.-P. Liu, K.-R. Chiou, V. J. Wedeen, T. G. Reese, and C.-F. Yang. Diffusion Tensor Magnetic Resonance Imaging Mapping the Fiber Architecture Remodeling in Human Myocardium After Infarction: Correlation With Viability and Wall Motion. *Circulation*, 114(10):1036–1045, 2006.[1]